

# Evaluation of Johnson-Cook Material Model Parameters of AA6063-T6

Devesh Rajput<sup>1</sup>, Ankit Singh<sup>2</sup>, Arpit<sup>3</sup>, Sanjay Kumar<sup>4</sup>

<sup>1,2,3</sup>Student, Mechanical Engineering Department, Delhi Technological University, Delhi, India

<sup>4</sup>Assistant Professor, Mechanical Engineering Department, Delhi Technological University, Delhi, India

\*\*\*

**Abstract** - The present work deals with the stimulus of strain rate on the behaviour of commercial aluminium alloy 6063-Temper 6. It is a medium strength alloy commonly referred to as architectural alloy and expected to have a low strain rate sensitivity. Consistent and judicious characterization of the material behaviour under the coupled effects of strain, strain rate, and temperature on the material flow stress is remarkably crucial to design as well as optimize the process parameters for industrial practice. Tensile tests were performed at room temperature at strain rates starting from  $10^{-4}$  to  $10^{-1}$  s<sup>-1</sup>. The alloy exhibited a low but positive strain rate dependence of material strength at the investigated strain rates. The stress-strain relations obtained through these tests were employed for calibrating Johnson-Cook (J-C) material model. An empirical constitutive relation stated by Johnson and Cook (J-C) is extensively used to capture the strain rate sensitivity of the metals. In this work, model constants of J-C constitutive relation have been determined experimentally from the uni-axial tensile test.

**Key Words:** Johnson-Cook, Material model, AA6063-T6, Strain rate, flow stress, ASTM – E8M.

## 1. INTRODUCTION

Aluminium alloys have developed as a strong candidate material for defence, aeronautical and automotive applications due to their low density, tremendous strength, and high corrosion resistance. But their mechanical behaviour has to be thoroughly understood to utilize their potential for such demanding applications. This requires a more profound understanding of the material properties, which is very complex due to the relationship between large plastic deformations, high strain rates, thermal softening as a result of adiabatic heating of materials, material deterioration, and fracture. The theory in continuum mechanics referred to as viscoplasticity [5] explains the rate-dependent inelastic response of solids. Rate-dependence in this setting means that the deformation of the material depends on the rate at which loads are employed.

Numerical techniques have surfaced as an efficient and cost-effective tool for investigating material behaviour. The reliability of numerical results depends massively on the exactness of material models used to interpret the dynamic behaviour of materials under consideration. The Johnson-Cook material model [1] is one of the most manageable models with five parameters, which can describe the material response at high temperatures, high strains, and high strain-rates and is often used in simulations. In addition

to the material model, a failure model introduced by Johnson and Cook is used to model the damage progression and foretell failure in many engineering materials.

## 2. LITERATURE SURVEY

Johnson and Cook (1983) suggested a simple model to describe the plastic behaviour of metals under dynamic loading. The model defines the equivalent flow stress as a function of strain, strain rate, and temperature.

$$\sigma_{eq} = (A + B\varepsilon_{eq}^n)(1 + C \ln \varepsilon_{eq}^{\dot{\varepsilon}})(1 - T^{*m}) \quad (1)$$

where  $A$  is Yield stress,  $B$  is Hardening modulus,  $C$  is Strain rate coefficient,  $n$  is Hardening exponent and  $m$  is thermal softening parameter. These are to be determined experimentally.  $\varepsilon_{eq}$  is equivalent plastic strain,  $\varepsilon_{eq}^{\dot{\varepsilon}}$  is the ratio of equivalent plastic strain rate to a reference plastic strain rate.  $T^*$  is the homologous temperature and is defined as

$$T^* = \frac{T - T_r}{T_m - T_r} \quad (2)$$

where  $T$  is the current temperature of the material,  $T_m$  is the melting temperature of material and  $T_r$  is room temperature. The first, second and third set of brackets in equation (1) picture the effect of isotropic strain hardening, strain rate hardening and thermal softening sequentially in an uncoupled manner.

Dislocation dynamics based material models like Zerilli-Armstrong model (1987) and Mechanical Threshold Stress model (Follansbee and Cocks 1988) have been introduced to judge linked nature of strain rate and thermal sensitivity but they have not been able to overtake Johnson-Cook (J-C) model due to complexity in the calibration of constants.

## 3. JOHNSON-COOK MATERIAL MODEL

A review study of material parameters of Johnson-Cook constitutive and failure model (Johnson and Cook 1983, 1985) for some regularly used aluminium alloys acknowledges that various researchers have obtained different parameters for the same alloy. Therefore, it is very important for researchers working in crucial areas to be self-governing in the calibration of dynamic material models.

### 3.1 Method for calibration of J-C material model

The fundamental concept in the quantification of J-C material model is to isolate the effect of strain hardening, strain rate hardening and thermal softening on the plastic behaviour of

the material. This can be accomplished by conducting mechanical tests under definite conditions of strain rates and temperatures. Cylindrical specimens are employed because of their axisymmetric nature.

### 3.2 Determination of Parameter A

Performed a tensile test as per ASTM E8M standard on a Universal Testing Machine (UTM) at room temperature (25°C) and at a reference strain rate ( $10^{-3} s^{-1}$ ). Parameter 'A' is the yield strength of the material, that can be found out by direct observation of the stress-strain curve for materials showing yield point phenomenon and by 0.2% strain offset method.

### 3.3 Determination of Strain Hardening Parameters B and n

If a tensile test is conducted at room temperature and  $10^{-3} s^{-1}$  strain rate, then both the second and third bracket of equation (1) simplifies to unity and gets reduced to the following form:

$$\sigma_{eq} = [A + B\varepsilon_{eq}^n] \tag{3}$$

For a uniaxial tensile test,  $\sigma_{eq} = \sigma$  and  $\varepsilon_{eq} = \varepsilon$

So, equation (3) can be written as

$$\sigma - A = B\varepsilon^n$$

Taking log on both sides:

$$\log(\sigma - A) = \log B + n \log \varepsilon \tag{4}$$

On excluding the elastic part of the stress-strain curve and plotting  $(\sigma - A)$  and plastic strain on a log-log plot. The slope of this curve represents the strain hardening exponent ( $n$ ) and the Y-intercept of the curve provides the strain hardening coefficient ( $B$ ).

### 3.4 Determination of Strain Rate Sensitivity Parameter C

Stress-strain curves at varying strain rates are needed at room temperature. Strain rates from  $10^{-4}$  to  $10^{-1} s^{-1}$  can be obtained using a conventional UTM by altering the cross-head speeds. One datum point from each of these stress-strain curves is chosen. This datum point resembles to the value of flow stress at a constant plastic strain before the onset of necking. Since all the experiments are performed at room temperature, the third bracket of equation (1) simplifies to

unity and it gets reduced to the following form:

$$\sigma = [A + B\varepsilon^n] \left[ 1 + C \ln \frac{\dot{\varepsilon}}{\dot{\varepsilon}_o} \right] \tag{5}$$

The reference strain rate ( $\dot{\varepsilon}_o$ ) is equal to  $10^{-3} s^{-1}$ . The term in first bracket of equation (5) corresponds to the quasi-static flow stress at the reference strain rate. Let this flow stress be represented as  $\sigma_o$ . Therefore, equation (5) can be rewritten as:

$$\frac{\sigma}{\sigma_o} - 1 = C \ln(10^3 \dot{\varepsilon}) \tag{6}$$

Now if the left-hand term of equation (6) is plotted against logarithm of strain rate multiplied by  $10^3$ , the slope of this curve will represent the strain rate sensitivity parameter.

## 4. MATERIAL AND METHODS

Extrusions of AA6063 are obtainable in various forms. Some of them are square box section, rectangular box section, equal angle, unequal angle, flat bar and tube section. 6063 is typically utilized for building hardware, architectural sections with good surface finish, medium strength furniture and anodized sections. Applications demanding higher strength typically use 6061 or 6082 instead.

### 4.1 Chemical Composition

The material under consideration was examined using ASTM E - 1251 test method and the Spectro analysis of the tensile specimen yielded result that complied to ASTM - 6063 specification.

Table -1: Spectroscopy results

Component	Wt. %
Silicon	0.504
Copper	0.0038
Magnesium	0.5476
Iron	0.163
Zinc	0.0087
Nickel	0.0028
Manganese	0.0139
Chromium	0.0016
Titanium	0.0213
Tin	<0.0010
Lead	0.0019
Vanadium	0.0091
Aluminium	98.71

### 4.2 Tensile specimen

Most specimens possess either a round or square standard cross-section with couple shoulders and a reduced section gauge length in between. The shoulders enable the specimen to be clamped while the gauge length shows the deformation and failure in the elastic region while it is stretched under

load. The specimen was fabricated following ASTM E8M specifications.

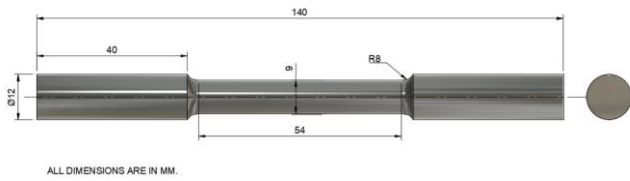


Fig -1: Dimensions of the tensile specimen

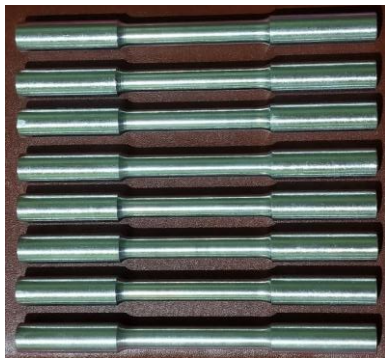


Fig -2: Tensile specimen

### 4.3 Experimental Setup

The experiments were carried out on the H50KS universal testing machine of TINIUS OLSEN ideal for high capacity tension testing. Tinius Olsen is the leading specialist fabricator and supplier of static tension and/or compression materials testing machines.

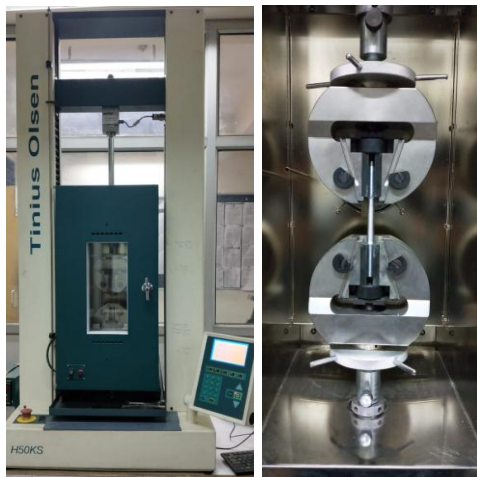


Fig -3: H50KS UTM

The strain rate used on a specimen has an extensive influence on the flow stress. It is expressed in units of per second. Uniaxial tension tests at strain rates ( $10^{-4}$  to  $10^{-1} s^{-1}$ ) were performed on H50KS UTM. Smooth cylindrical specimens of 9 mm gauge diameter were used.

$$\text{Strain rate} = \frac{\partial \epsilon}{\partial t} = \frac{\Delta L}{L \cdot \Delta T} = \frac{V}{L} \quad (7)$$

Where V is the cross-head velocity of the UTM,  $\Delta L$  and L depicts the change in length and original gauge length of the specimen. Tests were conducted at cross-head velocities of 0.27, 2.7, 27 and 270 mm/min, which correspond to strain rates of  $10^{-4}$ ,  $10^{-3}$ ,  $10^{-2}$  and  $10^{-1} s^{-1}$  respectively.

Engineering stress ( $\sigma_e$ ) and engineering strain ( $\epsilon_e$ ) were inferred from load and deformation history measured by the load cell and extensometer as follows:

$$\sigma_e = \frac{F}{A_0} \quad \epsilon_e = \frac{\Delta L}{L_0} \quad (9 \text{ and } 10)$$

The engineering stress-strain curve does not describe the real mechanical behaviour of the material as it is based on the original dimensions of the specimen.

True stress ( $\sigma_t$ ) and true strain ( $\epsilon_t$ ) in the specimen are based on instantaneous dimensions of the specimen and can be determined using the following relation :

$$\sigma_t = \sigma_e (1 + \epsilon_e) \quad (11)$$

$$\epsilon_t = \ln(1 + \epsilon_e) \quad (12)$$

The expressions of true stress and true strain are derived considering constant volume and steady deformation of the specimen along its gauge length.

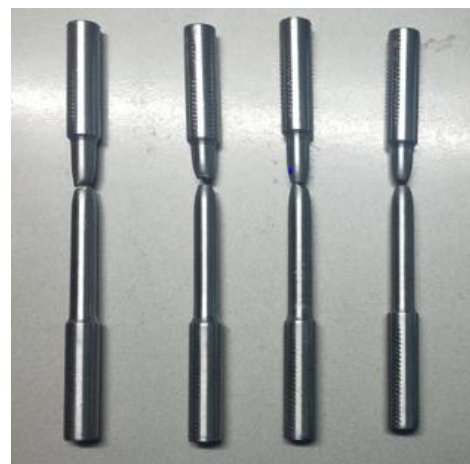


Fig -4: Fractured specimen

### 5. EVALUATION OF MATERIAL PARAMETERS FOR AA6063-T6

Fig -5 to Fig -8 distinguishes engineering and true stress-strain curves. The two curves are overlapping each other in the elastic region but begin deviating following the onset of plastic deformation. This is due to the fact that the engineering stress-strain curve is based on the original dimensions of the specimen whereas the true stress-strain curve is based on the instantaneous dimensions of the specimen. The engineering stress-strain curve attests to the fact that the stress almost remains constant in the plastic region as if the material is perfectly plastic but the true

stress-strain curve depicts the actual strain hardening behaviour of the material as there is a notable increase in stress with an increase in plastic strain. Therefore, all the engineering stress-strain curves were transformed into true stress-strain curves for discovering the constitutive relation for the material.

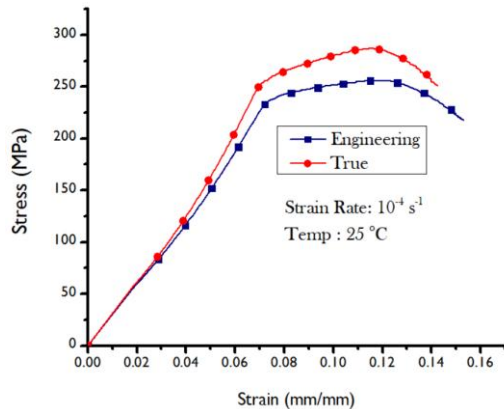


Fig -5: Engineering and True stress-strain curve for AA6063-T6 at strain rate  $10^{-4} \text{ s}^{-1}$ .

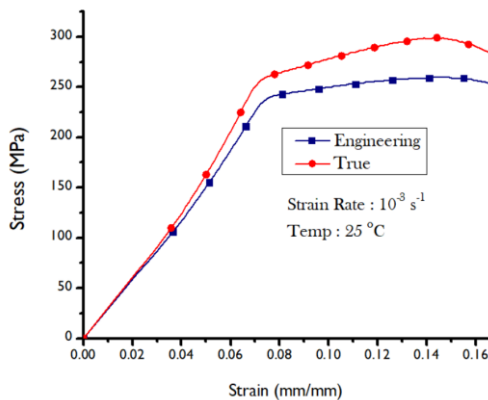


Fig -6: Engineering and True stress-strain curve for AA6063-T6 at strain rate  $10^{-3} \text{ s}^{-1}$ .

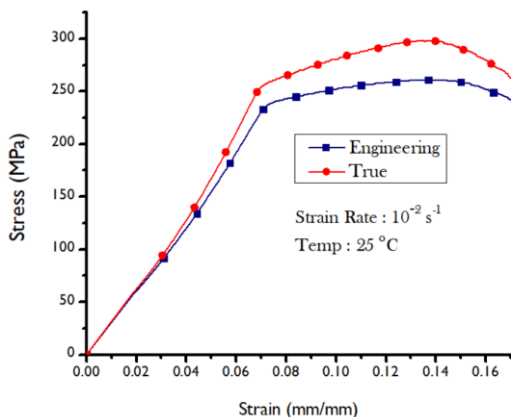


Fig -7: Engineering and True stress-strain curve for AA6063-T6 at strain rate  $10^{-2} \text{ s}^{-1}$ .

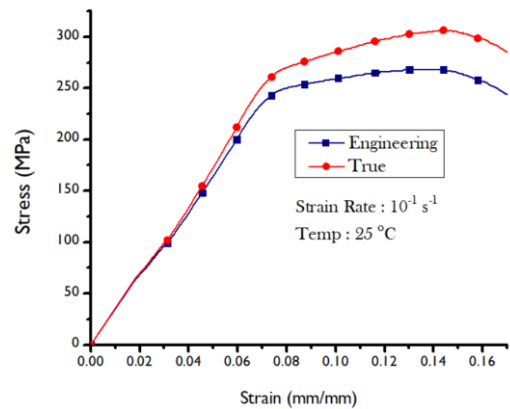


Fig -8: Engineering and True stress-strain curve for AA6063-T6 at strain rate  $10^{-1} \text{ s}^{-1}$ .

All these tests were conducted at room temperature ( $25^\circ\text{C}$ ). A couple of specimens were tested at each strain rate to ensure the uniformity of results. The material does not exhibit a well-defined yield point where the transformation from elastic to plastic behaviour takes place. Therefore, the 0.2 % offset strain method was adopted to determine the yield stress. A straight line is drawn parallel to the elastic curve at a 0.2 % strain offset. The intersection of this offset line with the stress-strain curve was considered as yield point and the corresponding stress value is known as yield stress of the material. This yield stress is equal to parameter A of the Johnson-Cook model.

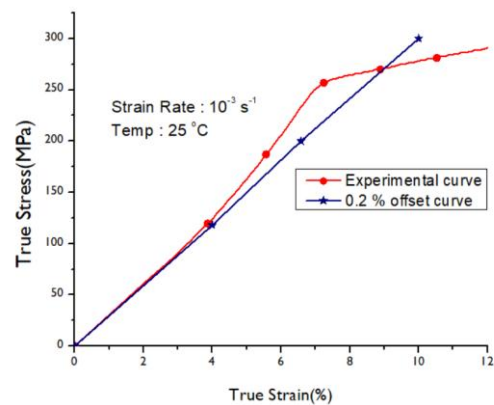
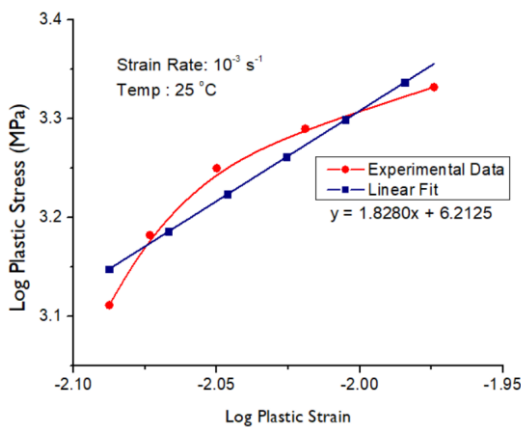


Fig -9: Determination of yield strength for AA6063-T6.

The strain hardening coefficient ( $B$ ) and strain hardening exponent ( $n$ ) are computed from Fig -10 employing the method elaborated in section 3.3. The plastic part of the stress-strain curve (at strain rate  $10^{-3} \text{ s}^{-1}$ ) is plotted on a log-log scale. The slope of this curve is equal to strain hardening coefficient ( $B$ ) and the exponential of Y-intercept gives stress hardening exponent ( $n$ ).



**Fig -10:** Determination of strain hardening parameters for AA6063-T6.

Strain sensitivity parameter ( $C$ ) is computed from Fig-11 as explained in section 3.4.

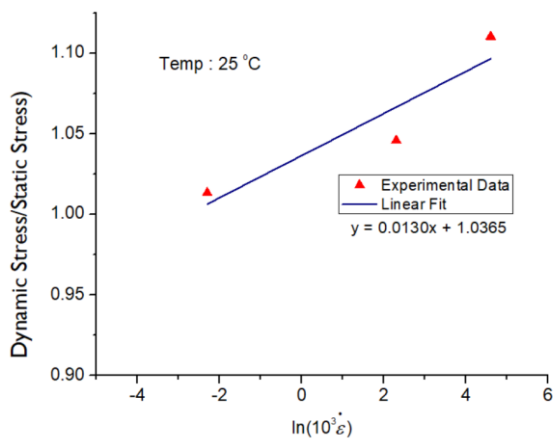


**Fig -11:** Determination of parameter ( $C$ ) for AA6063-T6.

The value of the thermal sensitivity parameter ( $m$ ) for AA6063-T6 is taken from the literature [4] as high-temperature tests could not be performed on the specimen.

**Table -2:** Johnson-Cook material model parameters for AA6063-T6.

$A$	$B$	$n$	$C$	$m$
270 MPa	498 MPa	1.8280	0.0130	1.003

## 6. CONCLUSIONS

In this study, we examined AA6063-T6 and obtained its tensile properties within a wide range of strain rates ( $10^{-4}$  to  $10^{-1} \text{ s}^{-1}$ ) under room temperature. The material displayed a positive strain rate dependence. Experimental results were utilized to discover dynamic yield stresses as well as constants of the Johnson-Cook equation.

The plastic behavior of a material can be explained using parametric material models such as the Johnson-Cook model. Obtained constants for AA6063 placed in Table-2 using this method are sufficient to be used in numerical simulations.

The Johnson-Cook material model is one of the most flexible models with five parameters, which can explain the material response at high temperatures, high strains, and high strain-rates. The increase in stress with strain rate is found to be irregular. This is maybe due to experimental error.

## ACKNOWLEDGEMENT

We express our deep sense of gratitude and indebtedness to our project guide Assistant Prof. Sanjay Kumar, Department of Mechanical Engineering, Delhi Technological University for introducing the topic to us and his constant supervision throughout the course of this work. We highly appreciate the help extended by Professor Vijay Gautam for furnishing us with required lab permissions. Our gratitude to Mr. Om Prakash for his help in conducting tensile tests in Applied Mechanics Lab. Finally, we would like to thank our parents for financing our education.

## REFERENCES

- [1] G.R. Johnson, W.H. Cook, A Constitutive Model and Data for Metals Subjected to Large Strains, High Strain Rates and High Temperatures, *Proceedings of the 7th International Symposium on Ballistics*, 1983.
- [2] Sharma, Prince & Chandel, Pradeep & Bhardwaj, Vikas & Singh, Manjit & Mahajan, Puneet. (2017). Ballistic impact response of high strength aluminium alloy 2014-T652 subjected to rigid and deformable projectiles. *Thin-Walled Structures*. 126. 10.1016/j.tws.2017.05.014.
- [3] Applied Impact Mechanics - Book by C. Lakshmana Rao, K. R. Y. Simha, and V. Narayanamurthy.
- [4] Kruszka, Leopold & Anaszewicz, Łukasz & Janiszewski, Jacek & Grazka, Michal. (2012). Experimental and numerical analysis of Al6063 duralumin using Taylor impact test. *EPJ Web of Conferences*. 26. 01062-10.1051/epjconf/20122601062.
- [5] Perzyna, P. (1966), "Fundamental problems in viscoplasticity", *Advances in Applied Mechanics*, 9 (2): 244–368.
- [6] Che, J., Zhou, T., Liang, Z. *et al.* An integrated Johnson–Cook and Zerilli–Armstrong model for material flow behavior of Ti–6Al–4V at high strain rate and elevated temperature. *J Braz. Soc. Mech. Sci. Eng.* 40, 253 (2018). <https://doi.org/10.1007/s40430-018-1168-7>.

## BIOGRAPHIES



### DEVESH RAJPUT

B.Tech. Final Year Student  
Dept. of Mechanical Engineering  
Delhi Technological University



**ANKIT SINGH**

B.Tech. Final Year Student  
Dept. of Mechanical Engineering  
Delhi Technological University



**ARPIT**

B.Tech. Final Year Student  
Dept. of Mechanical Engineering  
Delhi Technological University



**SANJAY KUMAR**

Assistant Professor  
Dept. of Mechanical Engineering  
Delhi Technological University